A Parameterization of Bowen Ratio with Respect to Soil Moisture Availability

Ye Zhuojia[①②] and *Roger A. Pielke*[②]

Received February 16, 1995; revised May 8, 1995

ABSTRACT

The Bowen ratio (B) is impacted by 5 environmental elements: soil moisture availabillity, m, the ratio of resistances between atmosphere and soil pores, $\frac{r_a}{r_D}$, atmospheric relative humidity, h, atmospheric stability, ΔT, and environment temperature. These impacts have been investigated over diverse surfaces, including bare soil, free water surface, and vegetation covered land, using an analytical approach. It was concluded that: (a) B is not a continuous function. The singularity exists at the condition $\alpha h_{cb} = h$, occurring preferably in the following conditions: weak turbulence, stable stratified stability, dry soil, and humid air, where h_{cb}, defined by Eq.(11) is a critical variable. The existence of a singularity makes the dependence of B on the five variables very complicated. The value of B approaches being inversely proportional to m under the conditions $m \geq m_{fc}$ (the soil capacity) and / or $\frac{r_a}{r_D} \rightarrow 0$. The proportional coefficient changes with season and latitude with relatively high values in winter and over the poles; (b) B is nearly independent of $\frac{r_a}{r_D}$ during the day. The impact of m on B is much larger as compared to that of $\frac{r_a}{r_D}$ on B; (c) when h increases, the absolute value of B also increases; (d) over bare soil, when the absolute surface net radiation increases, the absolute value of B will increase. The impact of R_N on B is larger at night than during the day, and (e) over plant canopy, the singularity and the dependcies of B on m, r_a, and h are modified as compared to that over bare soil. Also (i) during the daytime unstable condition, m exerts an even stronger impact on B; at night, however, B changes are weak in response to the change in m; (ii) the value of B is much more sensitive in response to the changes of turbulent intensity; (iii) the B response to the variation of h over a vegetation covered area is weaker; and (iv) the singularity exists at the condition $h_{cp} = h$ instead of $\alpha h_{cb} = h$ as over bare soil, where h_{cp} is defined by Eq.(49). The formulas derived over bare soil also hold the same when applied to free water bodies as long as they are visualized as a special soil in which the volumetric fraction of soil pore is equal to one and are fully filled with water. Finally, the above discussions are used to briefly study the impact on the thermally induced mesoscale circulations.

Key words: Bowen ratio parameterization, Soil moisture availability, Plant canopy

I. INTRODUCTION

The Bowen ratio, B, is defined as:

$$B = H_s / LE \ , \tag{1}$$

where H_s and LE are fluxes of sensible and latent, respectively, expressed in terms of resistance law as follows:

① Institute of Atmospheric Physics, Chinese Academy of Sciences, Beijing 100029, China
② Colorado State University, Department of Atmospheric Science, Fort Collins, Colorado 80523, USA

$$H_s = \rho c_p \frac{T_s - T_a}{r_H} \quad , \tag{2}$$

$$LE = \rho L \frac{q_s - q_a}{r_q} \quad , \tag{3}$$

where ρ is the density of the air, c_p is the specific heat at constant pressure, L is the latent heat per unit mass for evaporation or condensation, T is the temperature, q is the specific humidity, subscripts s and a stand for surface and air, respectively, and r_H and r_q are resistances to the exchange of sensible and latent heat, respectively. In the present study, $r_H = r_q = r_a$ is assumed, and it is defined as:

$$r_a = \int_0^{Z_a} \frac{1}{K_a} dZ \quad , \tag{4}$$

where K_a is the diffusivity of heat and water vapor by eddies and molecules. The values of H_s and LE can also be parameterized through the surface heat balance equation, as:

$$H_s = \frac{(1-\lambda)R_N}{1+B^{-1}} \quad , \tag{5}$$

$$LE = \frac{(1-\lambda)R_N}{1+B} \tag{6}$$

where $\lambda = G / R_N$ and R_N is the net radiation flux at surface and G is the heat flux from or to the earth. The value $\lambda = 0$ over a completely plant–shielded land, and $\lambda \leqslant 03$ over bare soil will decrease as m defined by Eq.(8) increases.

Equations (5) and (6) indicate that B determines the relative intensity of H_s and LE, partitioned from R_N.

The value of m over the earth is distributed heterogeneously by both the spatial and temporal variation of precipitation and as a result of human activities (such as irrigation). Increasing soil wetness will result in an increase of evaporation from bare soil and evapotranspiration from plants. That is to say that LE, partitioned from R_N, increases. Consequently, B is expected to decrease. The soil albedo over bare soil, A, decrease when m increases, which should cause a variation of solar heating with m, and is estimated by the following:

$$A = \max(A_{\min}, A_d - \alpha_m m), \tag{7}$$

where A_d is the value of A at $m = 0$, $A_{\min}$ is the minimum value of A at $m = m_c = \frac{A_d - A_{\min}}{\alpha_m}$, and m is defined as:

$$m = \eta_w / \eta_w^{sat} \quad , \tag{8}$$

where η_w is the actual soil volumetric water fraction, and η_w^{sat} is the value of η_w at saturated soil condition. For loamy soil, $A_{\min} = 0.14$, $A_d = 0.31$, and $\alpha_m = 0.34$ (Idso et al., 1975).

It is known that the mesoscale horizontal distribution in surface sensible heat flux is the basic physical factor to force thermally induced mesoscale circulations (TIMC) [Segal and Arritt, 1991]. The interest of investigating the impact of m on B lies in that the theoretical relationships between the intensities of TIMC and R_N as well as other environmental parameters (such as m) can explored as will be briefly discussed in Section 4 as the impacts of

these parmeters on B are known. Recently, many studies have been devoted toward experimentally studying B over different land areas (e. g., Table 1). However, to date, very few studies have been completed to theoretically investigate the impact of m on B. Segal et al. (1990) made a preliminary study on this subject from numerical simulation results. In that study, q_s is parameterized by Eq.(9) under the specific conditions:$\alpha = 1$ and $\beta = m_g$. The simulation results indicated that B is inversely proportional to m_g:

$$B = 0.06 + N_b m_g^{-1} \ ,$$

where $N_b = 0.2$ when the initial surface temperature at 10 m above the surface was set at 293 K for the summer case and 0.32 for the winter case (283 K). The subscripts g and b stand for the values at ground surface and under bare soil condition, respectively.

Table 1. Values of Bowen Ratio Derived from Field Experiments

Authors	B	land-use
Nunez and Oke (1977)	~6.4	urban canyon of Vancouver B.C.
Kalanda et al. (1980)	0.5~1.0	suburban of Vancouver B.C.
Oke (1982)	0.1~1.5	rural of Vancouver B.C.
	0.25~2.5	suburban of Vancouver B.C.
	0.5~>4	urban of Vancouver B.C.
Clengh and Oke (1986)	0.46	rural of Vancouver B.C.
	1.28	suburban of Vancouver B.C.
Ching et al. (1983)	0.8	rural of St. Louis
	2.1	city of St. Louis
Ching (1985)	<0.2	non-urban area of St. Louis
	>1.5	city of St. Louis
McCaughey (1985)	0.2~1.0	forest site in Ontario
	0.4~	clear-cut site in Ontario
Smith et al. (1986)	~10 (Spring)	Gobi desert, Gansu province China
	~0.35 (Summer)	Gobi desert, Gansu province China

It is the purpose of the current study to further explore the physical relationship between B and m, both over bare soil and over a plant canopy using an analytical approach. The impacts of atmospheric turbulent intensity characterized by r_a, atmospheric thermal stability and temperature on the Bowen ratio are also given special attention. The Bowen ratio over vegetation-covered areas is briefly discussed as well.

II. OVER BARE SOIL

Following Ye and Pielke (1993), the parameterization of q_s in Eq.(3) over bare soil is given by the form called the "α- and β-method":

$$q_s = \alpha\beta q_s^{sat} + (1-\beta)q_a \ , \tag{9}$$

where q_s^{sat} is the value of q_s at saturation condition. By setting $\beta = 1$ or $\alpha = 1$, Eq.(9) is

changed to the α– or β–method. Rearranging Eq.(9) yields:

$$q_s - q_a = \beta(\alpha q_s^{sat} - q_a) = \beta q_s^{sat}(\alpha - h h_{cb}^{-1}) \ , \tag{10a}$$

$$= \beta[(\alpha S(T_s - T_a) + (\alpha - h) q_s^{sat}] \ , \tag{10b}$$

$T_s - T_a$ in Eq.(2) can be expressed as:

$$T_s - T_a = \frac{q_s^{sat} - q_a^{sat}}{S} = \frac{q_s^{sat}}{S}(1 - h_{cb}^{-1}), \tag{10c}$$

where $h = q_a / q_a^{sat}$ is relative humidity, $S = dq^{sat} / dT$ is the slope of q^{sat} while changing T at constant pressure, and h_{cb} is a critical variable defined as:

$$h_{cb} = q_s^{sat} / q_a^{sat} \ . \tag{11}$$

The value of h_{cb} is determined by the temperature difference, $\Delta T = T_a - T_s$; $h_{cb} > 1$ corresponds to an unstable atmosphere, and $h_{cb} < 1$ for stable conditions. Substituting Eqs.(10a) and (10c) into Eqs.(3) and (2) results in:

$$H_s = \frac{\rho c_p}{r_a} \frac{q_s^{sat}}{S} \frac{h_{cb} - 1}{h_{cb}}, \tag{12}$$

$$LE = \frac{\rho L}{r_a} \beta q_s^{sat} \frac{\alpha h_{cb} - h}{h_{cb}} \ . \tag{13}$$

Substituting Eqs.(12) and (13) into Eq.(1) yields:

$$B = \frac{N_b}{\beta} \ , \tag{14}$$

where

$$N_b = \frac{c_p}{LS} \cdot \frac{h_{cb} - 1}{\alpha h_{cb} - h} \ . \tag{15}$$

Equations (11), (14), and (15) indicate that: (a) For a given value of N_b, B over bare soil is inversely proportional to β; (b) the proportional coefficient, N_b is a function with a singularity at $\alpha h_{cb} = h$. Based on Eq.(13) the sign of $\alpha h_{cb} - h$ determines whether LE is upward ($LE > 0$) or downward ($LE < 0$). Similarly, H_s is determined by $h_{cb} - 1$. (In a neutral atmospheric condition, $h_{cb} = 1$. For this case, based on Eq.(14), if $\alpha h_{cb} - h \neq 0$, which results in $N_b = 0$, $B = 0$.); (c) during the daytime in an unstable atmosphere (i.e., $h_{cb} > 1$ and $\alpha h_{cb} > 1$ is similar), B grows larger with a moistening atmosphere. At night in a stable stratified atmosphere (i. e., $h_{cb} < 1$), the dependence of B on h is complicated. $B > 0$ when $h > \alpha h_{cb}$. The impact of h on B is opposite to that found in daytime unstable atmospheric conditions. When $h < \alpha h_{cb}$, there is no water being condensed in the nighttime and the evaporation process continues. The value of B in this condition is negative and decreases as the value of h increases; (d) B will vary diurnally and seasonally because S and L depend on T, and h_{cb} depends on atmospheric thermal stability. Also the temperature and thermal stability change their values diurnally and annually.

A diversity of the parameterization for coefficients α and β has been presented as summarized in our previous paper (Ye and Pielke, 1993). Based on the discussion in that paper, it is preferable to use the new derivations in parameterizing α and β, where α and β are ex-

pressed as:

$$\beta = \chi_p(g)\beta_* \ , \tag{16}$$

$$\beta_* = 1 - \frac{1 - m_g}{1 + \frac{x_{p(1)}}{x_p(g)} \cdot \frac{1 - m_{(1)}}{1 - m_{(g)}} \cdot \frac{r_a}{r_D}} \ , \tag{17}$$

$$\alpha\beta_* = m_{(g)} + \frac{(1 - m_{(1)})\frac{x_{p(1)}}{x_{p(g)}}}{1 + \frac{x_{p(1)}}{x_{p(g)}} \cdot \frac{1 - m_{(1)}}{1 - m_{(g)}} \cdot \frac{r_a}{r_D}} \cdot \frac{r_a}{r_D} \cdot \frac{q^{sat}_{(1)}}{q^{sat}_{(g)}} \cdot h_s(m_{(1)}) \ , \tag{18}$$

where χ_p is the volumetric fraction of soil pores, r_D is the resistance to water vapor diffusion in the soil pores, and h_s is the relative humidity in the pores. The subscripts (g) and (1) stand for the values in a very thin upper soil layer, ΔZ_0, and within inner soil pores associated with a thin layer of depth ΔZ_1 next to the upper soil layer ΔZ_0. The value of h_s as dependent on m, is estimated using the formula given by Jacquemin and Noilhan (1990):

$$h_s(m) = \begin{cases} 05\left[1 - \cos\left(\frac{m}{m_{fc}}\pi\right)\right] & \text{if} \quad m < m_{fc} \\ 1 & \text{otherwise} \ , \end{cases} \tag{19}$$

where the subscript fc stands for soil field capacity. In the current study, all results presented are based on loamy sand soil with $m_{fc} = 0.366$ and $\chi_p = 0.41$ (Lee and Pielke, 1992).

1. *The Dependence of B on* $\frac{r_a}{r_D}$

The impact of atmospheric turbulent intensity measured by r_a on B over bare soil has rarely been discussed previously.

Figure 1 illustrates the impact of $\frac{r_a}{r_D}$ on B_* ($B_* = \chi_p B$) computed based on Eqs.(11) and (14) to (19) under the following conditions: $T_g = 304$ K, $\Delta T = T_a - T_g = -4$ K (unstable atmospheric stability), $h = 60\%$ (Fig.1a); and $T_g = 284$ K, $\Delta T = 4$ K (inversion), and $h = 71\%$ (Fig.1b). Three cases of m_g are computed: $m_g = 0.05$ (profile A representing dry soil), 0.25 (profile B, moisture soil) and 0.5 (profile C, wet soil) with the assumption that the values of temperature and moisture in the loamy sand soil are uniformly distributed in the vertical direction (this assumption will be used throughout this study).

Figure 1a shows that the value of B_* during the day is positive and approximately independent of $\frac{r_a}{r_D}$ when $\frac{r_a}{r_D}$ increases from 0.01 to 0.1 as shown by profiles B and C. When the soil tends to dry, the function of $B_*\left(\frac{r_a}{r_D}\right)$ may be involved in a singularity as shown by profile A, where the vertical line in the figure corresponds to a singularity which separates $B_* > 0$ from $B_* < 0$ at $r_a / r_D \approx 0.062$ in these given conditions. $B_* > 0$ is associted with strong atmosphere turbulent intensity. In contrast to profiles B and C, the absolute value and the profile slpoe in profile A are much larger. Therefore, strong turbulent intensity favors $B_* > 0$ even over very dry soil as shown in profile A.

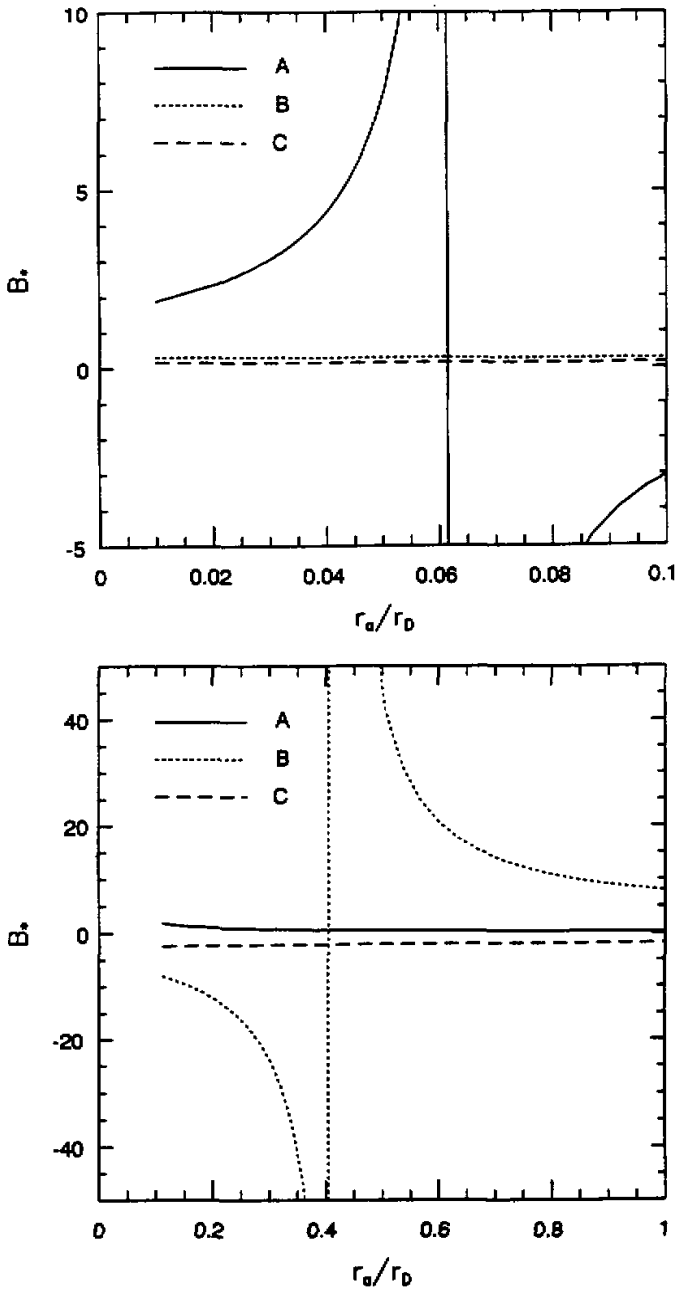

Fig. 1. B_* profiles ($B_* = X_p B$) as dependent on r_a / r_D over bare soil under the conditions: $T_g = 304$ K, $\Delta T = -4$ K, $h = 60\%$ (Fig. 1a) $T_g = 284$ K, $\Delta T = 4$ K, and $h = 71\%$ (Fig. 1b) for three cases of $m_g = 0.05$ (profile A) 0.25 (profile B) and 0.5 (profile C) with the assumption that both temperature and moisture in a loamy sand soil are uniformly distributed.

At night with weak turbulent conditions, Fig.1b illustrates that over wet soil (profile *C*), $B_* < 0$, but $B_* > 0$ while over dry soil (profile *A*). With a moist soil (profile *B*), B_* changes its sign from negative to positive when $\frac{r_a}{r_D}$ increases from 0.12 to 1.0, separated by a singularity at $\frac{r_a}{r_D} = 0.41$. Figure 1b also shows that negative values of B_* occur in favorable conditions over wet soil or over moist soil with relatively developed turbulent intensity. B_* decreases as $\frac{r_a}{r_D}$ increases.

The insensitive response of B_* to $\frac{r_a}{r_D}$ can be explained by examining the impact of $\frac{r_a}{r_D}$ upon α and β_*. Figure 2, computed based on Eqs.(17) to (19) under the same assumption given in Fig.1, shows that as $\frac{r_a}{r_D}$ increases, α decreases (when $m < m_{fc}$), but β_* increases. The contrary impacts of $\frac{r_a}{r_D}$ on α and β_* make the dependence of B_* on $\frac{r_a}{r_D}$ insensitive based on Eqs.(14) and (15).

The impact of $\frac{r_a}{r_D}$ on B_* can also be explored by differentiating Eqs.(14), (17), and (18) with respect to $\frac{r_a}{r_D}$ under the same assumption given in Fig.1, which results in:

$$\frac{dB_*}{d\left(\frac{r_a}{r_D}\right)} = \frac{B_*^2}{(h_{cb}-1)} \cdot \frac{LS}{c_p}\left[h\frac{d\beta_*}{d\left(\frac{r_a}{r_D}\right)} - h_{cb}\frac{d(\alpha\beta_*)}{d\left(\frac{r_a}{r_D}\right)}\right], \tag{20}$$

$$\frac{d\beta_*}{d\left(\frac{r_a}{r_D}\right)} = (1-m_g)\left[1+\frac{r_a}{r_D}\right]^{-2}, \tag{21}$$

$$\frac{d(\alpha\beta_*)}{d\left(\frac{r_a}{r_D}\right)} = (1-m_g)h_s\left[1+\frac{r_a}{r_D}\right]^{-2}. \tag{22}$$

Substituting Eqs.(21) and (22) into Eq.(20) yields:

$$\frac{dB_*}{d\left(\frac{r_a}{r_D}\right)} = B_*^2\frac{LS}{c_p}(1-m_g)\frac{h-h_{cb}h_s}{h_{cb}-1}\left[1+\frac{r_a}{r_D}\right]^{-2}. \tag{23}$$

Equation (23) indicates that (a) the slope of profile B_* is proportional to B_*^2 and inversely proportional to $\left(1+\frac{r_a}{r_D}\right)^2$. During the day, except for dry soil, B_* is small ($\sim 0(10^{-1})$) as shown by profiles *B* and *C* in Fig.1a. At night B_* is usually one order of magnitude larger than that during the day as seen by comparing Fig.1b with Fig.1a, which should result in the slope of the B_* profile at night being much larger as compared with that during

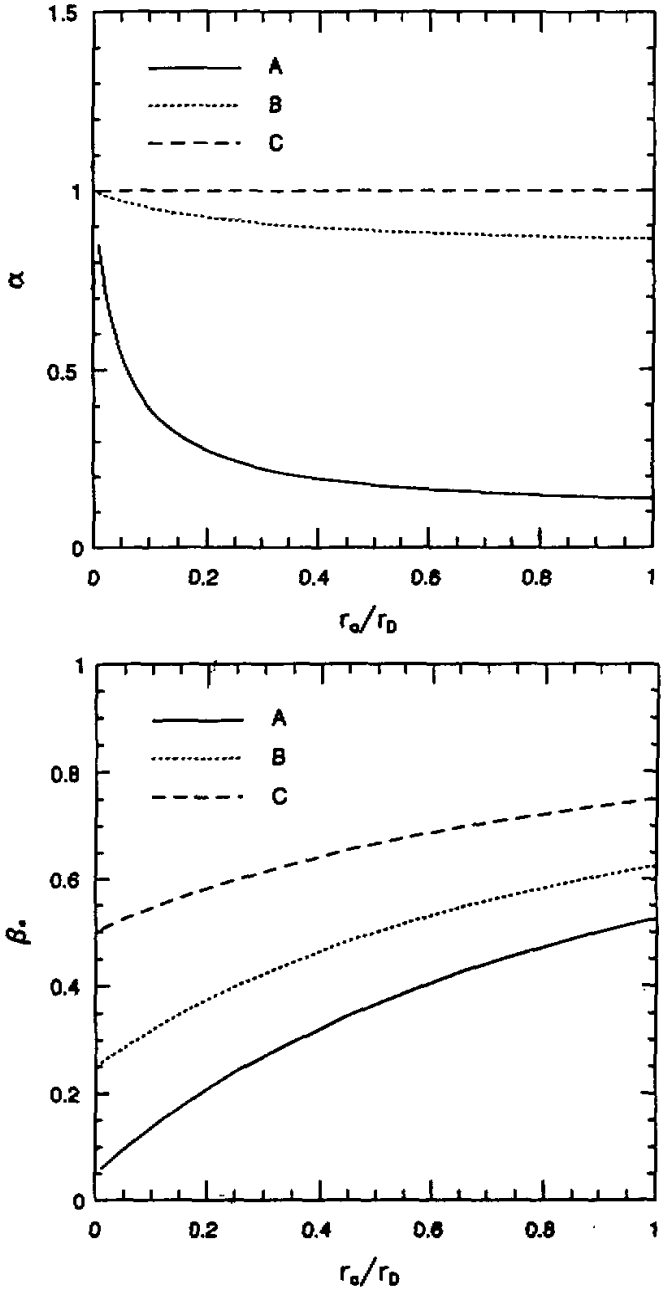

Fig. 2. α and β_* profiles as dependent on r_a / r_D for $m_g = 0.05$ (profile A), 0.25 (profile B), and 0.5 (profile C) under the same assumption as given in Fig. 1.

the day. However, since $\frac{r_a}{r_D}$ generally is one order or more larger at night than during the day, which will smooth the difference of the dependence of B_* on $\frac{r_a}{r_D}$ during the day from at night; (b) the slope $\frac{dB_*}{d\left(\frac{r_a}{r_D}\right)}$ is controlled by m_g. When m_g increases, the slope decreases with the assumptions that the other variables (h,h_{cb}, and $\frac{r_a}{r_D}$) are kept unchanged (as shown by Fig.1b, the slope is larger in profile A than profile C). when the soil is at saturated water content condition, $\frac{dB_*}{d\left(\frac{r_a}{r_D}\right)}=0$; and (c) the sign of $\frac{dB_*}{d\left(\frac{r_a}{r_D}\right)}$ depends on $\frac{h-h_{cb}h_s}{h_{cb}-1}$. Generally, at night $h_{cb}<1$ and $h>h_{cb}h_s$, which results in $\frac{dB_*}{d\left(\frac{r_a}{r_D}\right)}<0$ as shown by Fig.1b. During the day, $h_{cb}>1$, it is possible that $h>h_{cb}h_s$ for dry soil and $h<h_{cb}h_s$ over other soils. The former results in $\frac{dB_s}{d\left(\frac{r_a}{r_D}\right)}>0$ as shown by profile A in Fig.1a; the latter, $\frac{dB_*}{d\left(\frac{r_a}{r_D}\right)}<0$ as shown by profiles B and C (by careful investigation).

2. *The Dependence of B on* m_g

Figure 3 presents the impact of m_g on B_* computed from Eqs.(11) and (14) to (19) under the conditions $\Delta T=-4$ K, $T_g=304$ K, $h=60\%$, $\frac{r_a}{r_D}=0.1$ (profile A), and 0.01 (profile B) during the day (Fig.3a); and $\Delta T=4$ K, $T_g=284$ K, $h=71\%$, $\frac{r_a}{r_D}=1.0$ (profile A) and 0.1 (profile B) at night (Fig.3b), with the same assumptions as in Fig.1.

Figure 3a illustrates that during the day, $B_*>0$ except for the conditions $\frac{r_a}{r_D}=0.1$ and $m_g\leqslant 0.05$, where $B_*<0$. In contrast to the impact of $\frac{r_a}{r_D}$ on B_*, B_* is sensitive to the change in m_g, especially when $m_g<0.2$ in the loamy sand soil.

At night, Fig.3b shows that the singularity moves, respectively, to $m_g=0.22\left(\frac{r_a}{r_D}=0.1\right)$ and $0.27\left(\frac{r_a}{r_D}=0.1\right)$ instead of $m_g=0.05\left(\frac{r_a}{r_D}=0.1\right)$ during the day. It suggests that both $B_*>0$ and $B_*<0$ are possible at night with negative values of B_* corresponding to relatively large values of m_g.

The above features can be discovered by examining the dependence of α and β_* on m_g. Figure 4, computed based on Eqs.(17) to (19) under the same condition as that described in

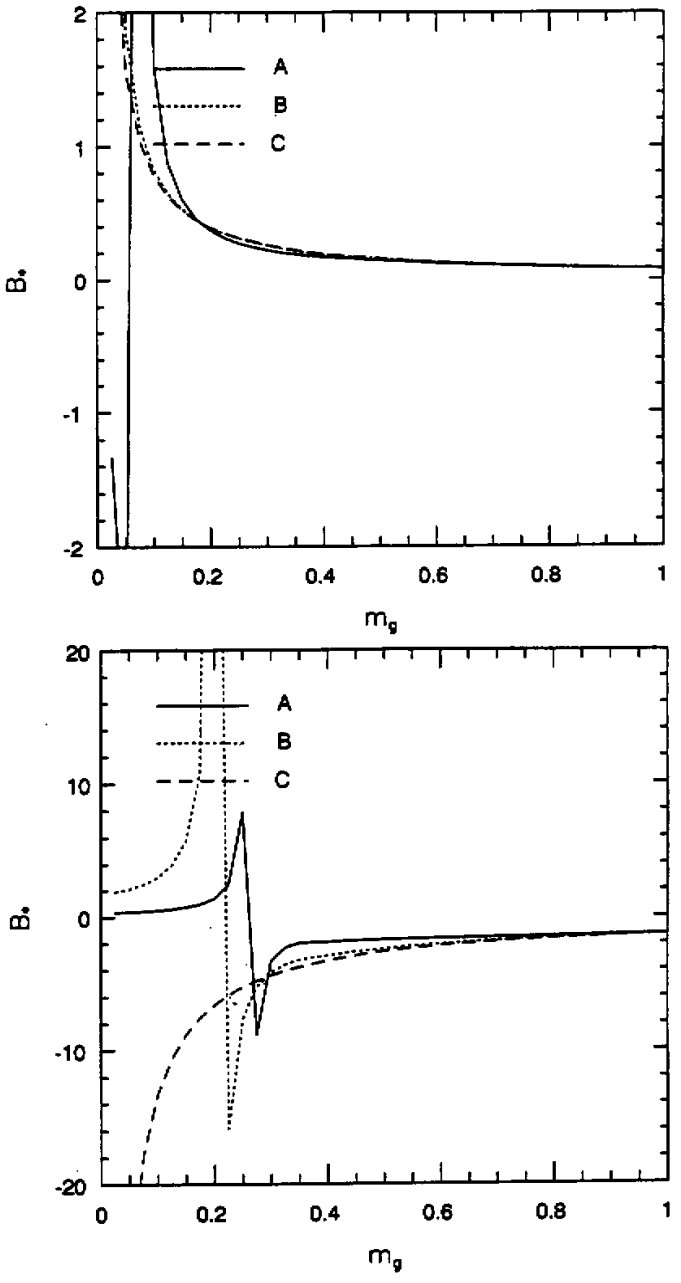

Fig. 3. The B_* profiles as dependent on soil moisture availability for bare soil condition (a) $T_g = 304$ K, $h = 60\%$, $\Delta T = -4$℃, $r_a / r_D = 0.1$ (profile A) and 0.01 (profile B) during the day (Fig. 3a); (b) $T_g = 284$ K, $h = 71\%$, $\Delta T = 4$℃, $r_a / r_D = 1.0$ (profile A) and 0.1 (profile B) at night (Fig. 3b) under the same assumptions as described in Fig. 1. Profile C are computed using a special β–method condition, i.e., the coefficients in Eq. (9), α and β, are set as $\alpha = 1$ and $\beta_* = m_g$.

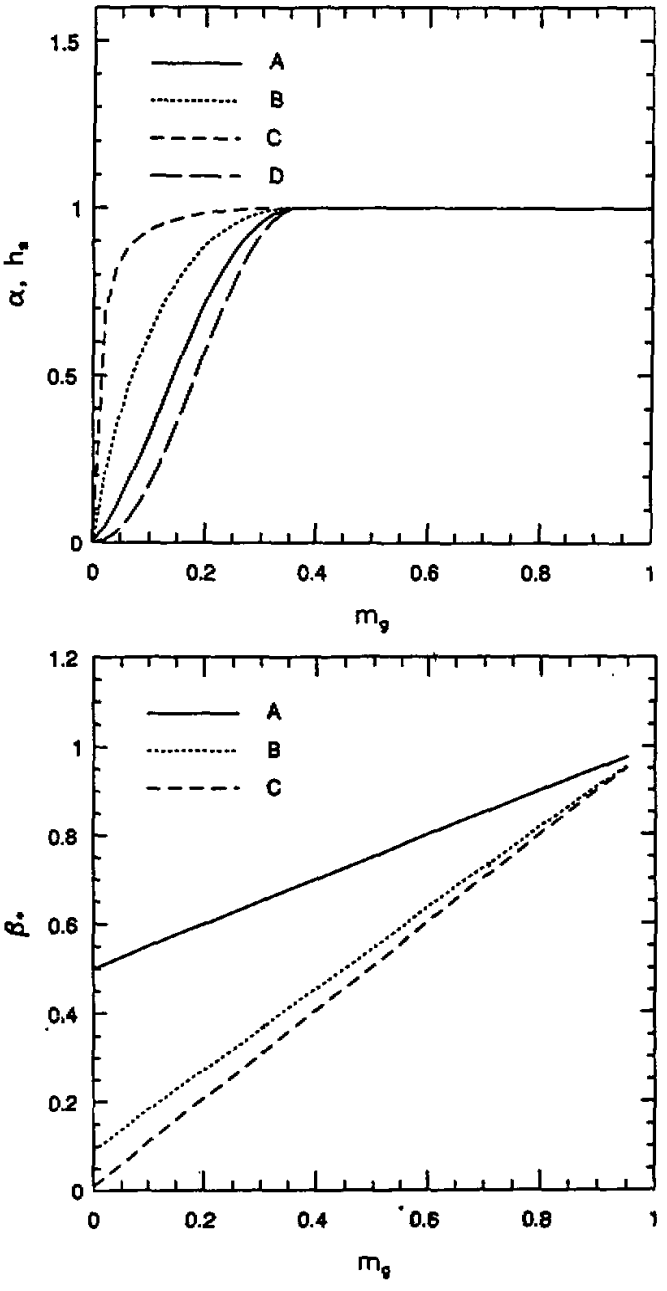

Fig. 4. α and β_* profiles as dependent on m_g for $r_u / r_D = 0.01$ (profile C), 0.1 (profile B), and 1.0 (profile A) under the same assumptions as given in Fig. 3.

Fig.3, shows that α and h_s (profile D in Fig. 4a) increase nonlinearly when m_g increases from 0 to m_{fc}, and $\alpha = h_s = 1$ when $m_g \geqslant m_{fc}$. Comparing profiles A, B and C with D in Fig.4a indicates that $\alpha \rightarrow h_s$ when $\frac{r_a}{r_D}$ is getting larger. The value of β_* is linearly increased as m_g increases under the given conditions. Both are responsible for the rapid decrease of B_* with m_g when $m_g < m_{fc}$ during the day and the sensitivity decreases after $m_g \geqslant m_{fc}$. The impact of m_g on B_* is stronger as compared with $\frac{r_a}{r_D}$ on B_*, because when m_g increases, α and β_* increase, however, when $\frac{r_a}{r_D}$ increases, β_* increases, but α decreases.

Profiles C in Figs.3a and 3b are computed in a special "β–method" condition, i.e., the coefficients in Eq.(9), α and β_* are set as:

$$\alpha = 1 \quad \text{and} \quad \beta_* = m_g \ . \tag{24}$$

Substituting Eq.(24) into Eqs.(14) and (15) results in the simplified formulas:

$$B_* = \frac{N_b}{m_g} \ , \tag{25}$$

$$N_b = \frac{c_p}{LS}\frac{h_{cb} - 1}{h_{cb} - h} \ . \tag{26}$$

Since N_b, expressed by Eq.(26), is independent of m_g, B is inversely proportional to m_g based on Eq.(25). Segal et al. (1990), from a set daytime numerical simulation results with the surface specific humidity parameterized also using Eq.(9) combined with the condition in Eq.(24), presented the same conclusion as that indicated by Eq.(25). In the following, specifications (24) are investigated and then under what conditions Eqs.(14) to (18) can approach Eqs.(24) to (26) and in what conditions B_* predicted from Eqs.(24) to (26) will significantly differ from that estimated from Eqs.(14) to (18) are discussed.

As illustrated by Fig.2a and 4a, $\alpha = 1$ (i. e., β–method holds in parameterizing q_s) occurs when $m_g \geqslant m_{fc}$ and $\alpha \rightarrow 1$ when $m_g \rightarrow m_{fc}$ or $\frac{r_a}{r_D} \rightarrow 0$. Figure 4b indicates that $\beta_* \approx m_g$ when $\frac{r_a}{r_D} \rightarrow 0$ ($\frac{r_a}{r_D} < 0.05$ as shown by profile C). It suggests that the necessary condition that makes Eq.(24) valid is $\frac{r_a}{r_D} \rightarrow 0$. Otherwise, Eq.(24) will deviate from Eqs.(16) to (18) even in the condition $m_g \geqslant m_{fc}$ because under this condition, $\alpha = 1$, but β_* deviates from m_g. The deviation of β_* from m_g increases as $\frac{r_a}{r_D}$ increases. These issues suggest that (a) when $\frac{r_a}{r_D} \rightarrow 0$ (it holds during the daytime in an unstable surface layer atmosphere), B_* predicted by Eqs.(25) and (26) is nearly exactly the same as that predicted by Eqs.(14) to (19) as illustrated in Fig.3a by profiles B computed from Eqs.(14) to (18) and C computed based on Eqs.(24) to (26) which shows that they nearly overlap each other with $N_b = 0.08$, and (b) when $m_g \geqslant m_{fc}$, Eq.(15) is equal to Eq.(26). As $\frac{r_a}{r_D}$ increases the deviation of β_*

from m_g also increases (see Fig.2b). Therefore, the difference of profile B_*, computed based on Eqs.(14) to (18), from that based on Eqs.(24) and (26) also increases as shown by comparing profiles A, B and C in Fig. 3. the difference is even more pronounced when $m_g < m_{fc}$. The reason is that the deviations of β_* from m_g and α from 1 increases as $\frac{r_a}{r_D}$ increases and / or m_g decreases as presented by Figs.2 and 4.

The above discussion suggests that a parameterization of surface specific humidity deviating from q_a, expressed by:

$$q_s - q_a = \chi_p m_g (q_s^{sat} - q_a) \tag{27}$$

which with $\chi_p = 1$ is commonly used in numerical model simulations, is not always suitable especially at night in weak atmospheric turbulent conditions. During the daytime, however, it does provide a very good prediction of B_*. Therefroe Eqs.(24) to (26) are the special cases of Eqs.(14) to (19) during the daytime condition.

3. *The Upper Bound on B_* During the Day*

As indicated in subsection 2.2 and illustrated Figs.2 (a and b), $\alpha \rightarrow 1$ and $\beta_* \rightarrow m_g$ during the day in an unstable atmosphere. From Eqs.(14 to 16) we have:

$$B = \frac{c_p}{LSm_g\chi_p}\frac{h_{cb}-1}{h_{cb}-h}. \tag{28}$$

When soil pores are completely filled with water and air is at a saturated condition, from Eq.(28), the upper bound on B can be derived as:

$$B_{\max} = \frac{c_p}{LS\chi_p}. \tag{29}$$

Equation (29) indicates that $B_{\max}$ is dependent on the soil texture. $B_{\max}$ for sand soil ($\chi_p = 0.395$) can be over two times as large as for peat soil ($\chi_p = 0.863$).

A free open evaporating water body can be visualized as a special soil in which there is no solid particles at all (i. e., $\chi_p = 1$) and all space is filled by water (i.e., $m = 1$). Equation (29) simplifies as Philip's equation (1987).

Philip (1987) indicated that above an evaporating water surface (such as lakes, for example) there is fixed an upper bound on B; thus $B_{\max}$ can be expressed as:

$$B_{\max} = \frac{c_p}{LS}. \tag{30}$$

4. *The Impact of Temperature on B*

The dependence of B_* on T_g is illustrated in Fig.5a computed from Eqs.(11) and (14) to (19) under the conditions: $\frac{r_a}{r_D} = 0.01, h = 60\%, m_g = 0.2$ (profile A) and 0.4 (profile B), $\Delta T = -4$ K during the day; and $\frac{r_a}{r_D} = 1.0, h = 71\%$, $m_g = 0.2$ (profile C) and 0.4 (profile D), $\Delta T = 4$ K at night. Figure 5a illustrates that the absolute value of B_* decreases when temperature increases. The impact of T_g on B_* is larger at night than during the day. The variation of temperature can be caused by variations of latitude, altitude, and season. Therefore, B

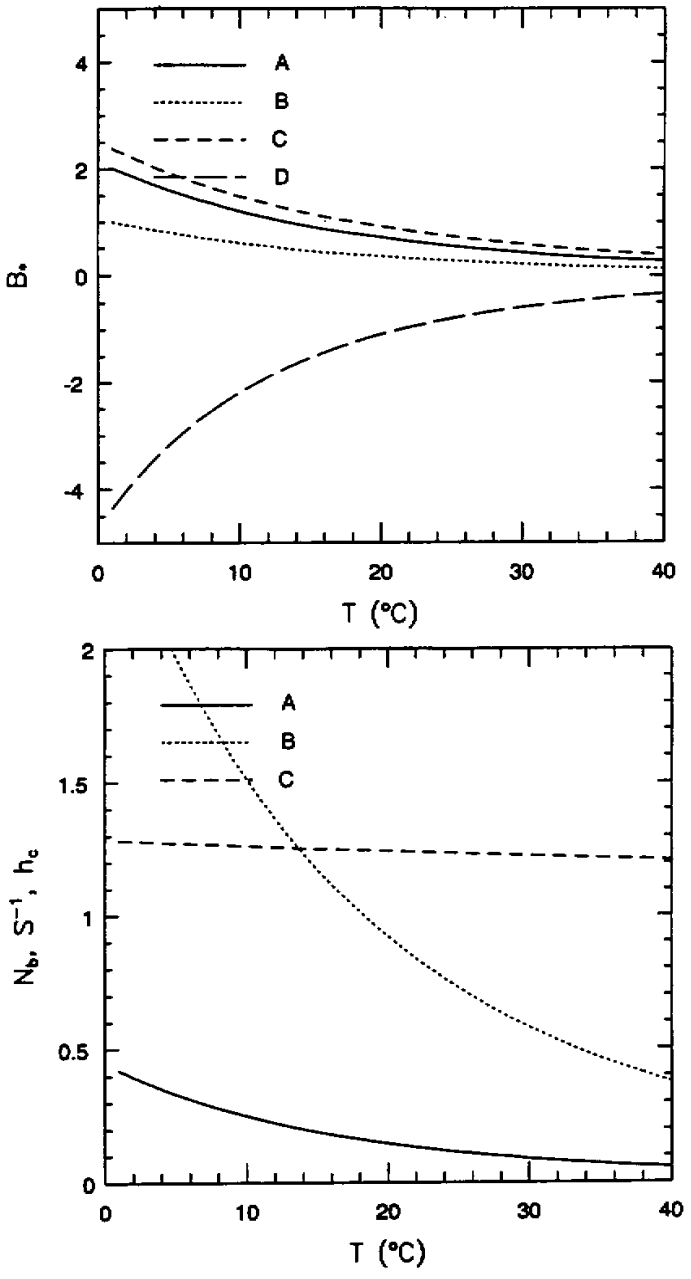

Fig. 5. (a) The impact of air temperature on B_* under unstable surface layer conditions: $r_a / r_D = 0.01$, $\Delta T = -4$ K, $h = 60\%$, $m_g = 0.2$ (profile A) and 0.4 (profile B) stable conditions: $r_a / r_D = 1.0$, $\Delta T = 4$ K, and $h = 71\%$, $m_g = 0.2$ (profile C) and 0.4 (profile D); (b) the dependence of S^{-1}(profile B), h_{cb} (profile C) and N_b (profile A) on T under the same conditions as given in (a).

has an annual cycle with a maximum in winter, and B changes with latitude and altitude, obtaining relatively large values in the polar areas and high mountain areas if the other conditions are kept the same. Segal et al. (1990), based on numerical model simulations during the day, presented the following results: B is inversely proportional to m_g, the proportionality is 0.2 for the summer case and 0.32 for the winter case with the simulation initial surface temperature in summer equal to 293 K and in winter, 283 K yielding a ratio of B (1.6) for the 10 K temperature departure. The analytical results produce profiles A and B in Fig.6a for the same temperature interval which is also 1.6. The above discussion indicates that part of our analytical results are supported by the numerical model simulations.

The values of L,S, and h_{cb} in Eq.(15) are temperature dependent variables, which are responsible for the alternation of B with T. Figure 5b presents the dependencies of S^{-1} (profile B), h_{cb} (profile C), and N_b (profile A) on T. The latter combines the impact of T on S^{-1},h_{cb}, and L. The dependence of L on T can be formulated as:

$$L = 597 - 0.57(T - 273.2)[T \quad \text{in} \quad K]. \tag{31}$$

Figure 5b and Eq.(31) indicate that the dependence of the slope of q^{sat} at constant pressure on T is responsible for the temperature dependence of the Bowen ratio, since values of N_b and S^{-1} are 7 times as large at $T = 274$ K as at $T = 312$ K according to our computational results.

5. *The Impact of Atmospheric Thermal Stability on B*

It is evident that H_s depends on atmospheric thermal stability measured by ΔT, but the dependence of LE on ΔT sometimes may be neglected. The impact of ΔT on LE is through the relation of h_{cb} with ΔT as expressed by Eqs.(11) and (13). In the following, a qualitative exploration of the slope of B_* with respect to ΔT will be drawn by differentiating Eq.(15) with respect to ΔT:

$$\frac{\partial B_*}{\partial \Delta T} = \frac{\beta_* \dfrac{\partial N_b}{\partial \Delta T} - N_b \dfrac{\partial \beta_*}{\partial \Delta T}}{\beta_*^2} \tag{32a}$$

with

$$\frac{\partial N_b}{\partial \Delta T} = \frac{c_p}{LS}\left[(\alpha - h)\frac{\partial h_{cb}}{\partial \Delta T} + (h_{cb} - 1)\left(\frac{\partial h}{\partial \Delta T} - h_{cb}\frac{\partial \alpha}{\partial\left(\dfrac{r_a}{r_D}\right)}\frac{\partial\left(\dfrac{r_a}{r_D}\right)}{\partial \Delta T}\right)\right] \Big/ (\alpha h_{cb} - h)^2 \ , \tag{32b}$$

and

$$\frac{\partial \beta_*}{\partial \Delta T} = \frac{\partial \beta_*}{\partial\left(\dfrac{r_a}{r_D}\right)}\frac{\partial\left(\dfrac{r_a}{r_D}\right)}{\partial \Delta T} \ . \tag{32c}$$

The orders of magnitude of $\dfrac{\partial h_{cb}}{\partial \Delta T}$, $\dfrac{\partial h}{\partial \Delta T}$, $\dfrac{\partial \alpha}{\partial (r_a / r_D)}$, and $\dfrac{\partial\left(\dfrac{r_a}{r_D}\right)}{\partial \Delta T}$ are considered as follows:

$\frac{\partial h_{cb}}{\partial \Delta T} \sim 0(10^{-2})$ and $\frac{\partial h_{cb}}{\partial \Delta T} < 0$ based on the estimation from Eq.(11). h_{cb} ranges from 0.32 at $\Delta T = 19$ K (very strong stability) to 2.7 at $\Delta T = -19$ K (very strong instability) $\frac{\partial h}{\partial \Delta T} \sim 0(10^{-2} \sim 10^{-3})$ The impact of ΔT on h is based on the following considerations: when ΔT change its value and sign, from positive to negative, for example, turbulent motion intensifies and the boundary layer deepens. As a result, the value of h decreases in response to the enhanced turbulent mixing between humid surface air and relatively dry elevated air. These features have been investigated in detail by Segal et al. (1992). $\partial \alpha / \partial \left(\frac{r_a}{r_D} \right)$ changes from 0 (10^{-1}) for dry soil to 0 when $m_g \geq m_{fc}$ based on Fig.2a; $\partial \beta_* / \partial \left(\frac{r_a}{r_D} \right)$ ranges from 0.5 ($m_g = 0.05$) to 0.25 ($m_g = 0.5$) based on Fig.2b; and $\partial \frac{r_a}{r_D} / \partial \Delta T \sim 0(10^{-2})$. According to these analyses, Eq.(32b) can be simplified as:

$$\frac{\partial N_b}{\partial \Delta T} \approx N_b \frac{(\alpha - h)}{(\alpha h_{cb} - h)(h_{cb} - 1)} \frac{\partial h_{cb}}{\partial \Delta T} , \tag{32d}$$

and $\beta_* \frac{\partial N_b}{\partial \Delta T}$ is one order of magnitude or more larger than $N_b \frac{\partial \beta_*}{\partial \Delta T}$. Therefore, Eq.(32a) simplifies to:

$$\frac{\partial B_*}{\partial \Delta T} \approx \frac{\partial N_b}{\partial \Delta T} / \beta_* \tag{33}$$

Equations (32d) and (33) indicates that during the daytime, generally $\alpha > h$ and $h_{cb} > 1$, thus $\frac{\partial N_b}{\partial \Delta T} < 0$ (i.e., $\frac{\partial B}{\partial \Delta T} < 0$) except over very dry soil which involves $\alpha < h$ but $\alpha h_{cb} > h$; in this case, $\frac{\partial N_b}{\partial \Delta T} > 0$. At night, $h_{cb} < 1$, therefore both $\alpha > h$ and $\alpha < h$ are possible. If $\alpha > h$ two situations can occur: $\alpha h_{cb} > h$ and $\alpha h_{cb} < h$. When $\alpha h_{cb} < h$, then $\frac{\partial N_b}{\partial \Delta T} < 0$ otherwise $\frac{\partial N_b}{\partial \Delta T} > 0$. If $\alpha < h$, consequently, $\alpha h_{cb} < h$, which occurs over very dry soil, therefore, $\frac{\partial N_b}{\partial \Delta T} > 0$.

Figure 6 shows an example to illustrate the impact of ΔT on B_* computed under the conditions: $m_g = 0.05$ (profile A), 0.25 (profile B), and 0.5 (profile C), and $T_g = 292$ K with the following consideration: when ΔT changes its value from $\Delta T = 19$K (very strong stability), to $\Delta T = -19$ K (very strong instability), the values of h and atmospheric turbulent intensity will be adjusted correspondingly. In the current study, h is set to 80% and $r_a / r_D = 1.0$ when $\Delta T = 19$ K and they will linearly decrease to $h = 42\%$ and $r_a / r_D = 0.01$ when $\Delta T = 19$ K.

Figure 6 illustrates that function $B_*(\Delta T)$ is discontinuous with singularities located at $\Delta T = -5$ K, 4 K and 6 K, rspectively for $m_g = 0.05, 0.25$, and 0.5, indicating that the value of ΔT at the singularity increases as m_g increases. The singularity separates evaporation from condensation processes: when ΔT is below this threshold, evaporation continues; above it, however, condensation occurs. Negative ΔT along with evaporation or positive ΔT along with condensation corresponds to $B_* > 0$. Otherwise the conditions correspond to $B_* < 0$.

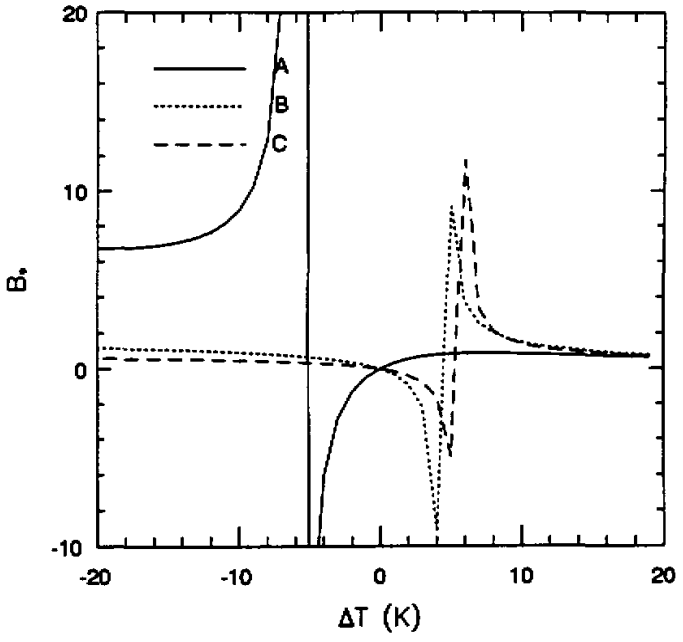

Fig. 6. The impact of ΔT on B_* for three cases of $m_s = 0.05$ (profile A), 0.25 (profile B) and 0.5 (profile C) with the same assumption as described in Fig. 1.

6. *The Impact of R_N on B*

In order to investigate the impact of the variation of R_N on B, a new formula of B is derived from Eq. (10b) as follows.

Equation (10b), divided first by $q_s - q_a$, then combining the resulting expression with Eqs. (1), (3), and (6), and reorganizing, results in:

$$B = \frac{\frac{1}{\beta} - N_1}{\frac{\alpha L S}{C_p} + N_1}, \tag{34}$$

$$\text{where} \quad N_1 = \frac{\rho L(\alpha - h) q_a^{sat}}{(1-\lambda) R_N r_a}. \tag{35}$$

Equation (35) indicates that the sign of N_1 is dependent on both $(\alpha - h)$ and R_N: $R_N > 0$ during daytime and $R_N < 0$ at night. Equation (34) shows that generally, the value of B is positive during the day because $\beta^{-1} > N_1 > 0$. At night however, the sign of B is determined by the relative values of $\alpha \frac{L}{c_p} S$ and N_1: $B < 0$ when $\alpha \frac{L}{c_p} S < |N_1|$, and, $B > 0$ otherwise. The dependence of α and β on m has been discussed in subsection 2.2. Now, the dependence of R_N on m during the day will be derived in the following. The solar radiation energy absorbed by a ground surface on bare soil can be expressed as:

$$R_S = S_o(1 - A), \tag{36}$$

where S_o is the incoming solar radiation flux at the ground surface and A is described by Eq. (7).

Inserting Eq. (7) into Eq. (36) results in:

$$R_S = R_{Sd} + \alpha_S \cdot \min(m, m_c), \tag{37}$$

where R_{Sd} is the value of R_S at the absolute dry soil condition, and α_S is a proportional coefficient, expressed as:

$$R_{Sd} = (1 - A_d)S_0, \tag{38}$$

$$\alpha_S = \alpha_m S_0. \tag{39}$$

Equation (37) suggests that the solar energy absorbed by the bare soil surface is linearly proportional to the soil moisture availability when $m \leqslant m_c$. In the following discussion, we focus on the condition $m \leqslant m_c$. The proportional coefficient, α_s is strongly dependent on S_o which is determined by solar day, latitude and local time and is about half of R_{Sd} for loamy soil. In a mid-latitude summer day at the noon hour under cloudless conditions, $R_{Sd} \approx$ 800 W m^{-2} and $\alpha_S \approx 400$ W m^{-2}.

R_N can be expressed as:

$$R_N = R_S + R_L^{\downarrow} - R_L^{\uparrow}, \tag{40}$$

where the downward longwave radiation flux, $R_L^{\downarrow}$ from a clear sky can be expressed by a empirical formula $R_L^{\downarrow} = \varepsilon_a \sigma T_a^4$, where ε_a depends on specific humidity and has a representative value about 0.4~ 0.5. $R_L^{\uparrow}$ is a longwave radiation flux emitted from the soil surface, $R_L^{\uparrow} = \varepsilon_g \sigma T_g^4$.

Differentiating Eq. (40) with respect to m and neglecting the impact of m on ε_g yields:

$$\frac{\partial R_N}{\partial m} = \alpha_s - \frac{4R_L^{\downarrow}}{T_a}\left(\frac{\varepsilon_g}{\varepsilon_a}\alpha_T^{-4} - 1\right)\frac{\partial T_a}{\partial m}, \tag{41}$$

where $\alpha_T = T_a / T_g$. An analysis on the order of magnitude of α_s and $\frac{4R_L^{\downarrow}}{T_a}\left(\frac{\varepsilon_g}{\varepsilon_a}\alpha_T^{-4} - 1\right)\frac{\partial T_a}{\partial m}$ suggests that the former is [10^2], and the latter [10^0~ 10^1] based on the following consideration: $T_a \approx [10^2]$ in K, α_T and $\frac{\varepsilon_g}{\varepsilon_a} \approx [10^0]$, $R_L^{\downarrow} \approx [10^2]$ in W m^{-2} and $\frac{\partial T_a}{\partial m} \sim [10^0]$. As a first approximation, the second term on the right-hand side of Eq. (41) can be neglected as compared to the value of α_S. Therefore, we have:

$$R_N = R_{Nd} + \alpha_S m, \tag{42}$$

where R_{Nd} is the value of R_N at a soil condition with $m = 0$. Comparing Eq. (42) with Eq. (37) indicates that the variations of R_N and R_s with m behave nearly the same. The reason seems that when the soil temperature decreases caused by the increase of soil moisture availability, the air temperature within the planetary boundary layer is also decreased proportionally. Therefore, the impact on m on $R_L^{\downarrow} - R_L^{\uparrow}$ becomes less important as compared to the impact

of m on R_S during the day. The impact of m on R_N at night is complicated and small (therefore it can be neglected) as compared to that during the day. Finally, the dependence of B on m formulated by Eq. (34) can be determined by Eqs. (16) to (19) and (42).
From Eq. (34) we have:

$$dB = -\left[\left(\frac{1}{\beta}+\frac{\alpha L}{c_p}S\right) / \left(\frac{\alpha L}{c_p}S+N_1\right)^2\right] dN_1 . \tag{43}$$

Equation (43) suggests that during daytime and at night, the absolute value of B will decrease when the absolute value of N_1 increases.This means that the increase of $|R_N|$ will result in the increase of $|B|$. During the day ($R_N>0$) when R_N increases, the atmospheric heating also increases, which forces an increase of the turbulent intensity near the surface (i.e., a decrease of r_a). This feature can weaken the dependence of N_1 (or B) on R_N based on Eq. (35). At night ($R_N<0$), when $|R_N|$ increases, r_a, also, increases. This feature strongly enhances the impact of R_N on B at night.

III. OVER PLANT-COVERED LAND

Over land cmpletely shielded by vegetation, the latent heat flux can be expressed as:

$$LE = \rho L \frac{q_p^{sat} - q_a}{r_a + r_s} . \tag{44}$$

The Bowen ratio can be derived from Eq. (44) using a similar procedure as that used over bare soil. The Bowen ratio is finally derived as:

$$B = \left(1+\frac{r_s}{r_a}\right) N_p , \tag{45}$$

where N_p is expressed by:

$$N_p = \frac{c_p}{LS}\left(\frac{h_{cp}-1}{h_{cp}-h}\right), \quad \text{and} \tag{46}$$

$$h_{cp} = q_p^{sat} / q_a^{sat} . \tag{47}$$

The subscript p stands for the plant canopy, the humidity at the leaf surface within the plant canopy is assumed to be at a saturated condition. r_s is the resistance of leaf stomata against vapor transpiration. Comparing Eq. (45) with Eqs. (14) and (15) under the conditions: $\alpha=\beta=1$, which expresses B over a free water surface, suggests that over completely vegetation covered land, B is larger than that over a free water body by a factor $\left(1+\frac{r_s}{r_a}\right)$. When $\frac{r_s}{r_a} \ll 1$, which can occur under special situations, for example, during the daytime (i.e., r_s is small) when warmer air moves over a cold surface, the B value over a canopy approaches that over free open water bodies. Generally, r_s and r_a are on the same order of magnitude, therefore, the Bowen ratio over vegetation covered land is larger than that over a free water body. The value of r_s depends on soil moisture availability and other environment variables such as solar radiation intensity, S_0, air temperature, T_a, saturation deficit of the environment humidity, $q_a^{sat} - q_a$, and CO_2 concentration. Parameterization formulations of r_s have been previously presented. It is difficult to compare the relative advantage among them. In the current

study, for the sake of simplification, the dependence of r_s on m and S_0 is adopted from Deardorff (1978), and the dependence of r_s on other environmental variables is taken from Singh et al. (1985), which yield a formulation of r_s as follows:

$$r_s = r_o \left(\frac{1+0.5LAI}{LAI}\right)\left[\frac{800}{1+S_0}+\left(\frac{c_1}{m}\right)^2\right]\left[\frac{e_a^{sat}(1-h)}{T_a}-C_2\right], \tag{48}$$

where a uniform distribution of m in the soil is assumed. $c_1 = 1.2\ m_{wilt}$, where m_{wilt} is a value of m at the plant state where it is at its wilting point. LAI is the leaf area index. C_2 is a constant, depending on plant type and plant structure. Combining Eqs. (45) and (48) results in:

$$B = N_p\left[1+A_p\left(\frac{800}{1+S_0}+\frac{c_1^2}{m^2}\right)\right], \tag{49}$$

$$\text{where}\quad A_p = \frac{r_o}{r_a}\left(\frac{1+0.5LAI}{LAI}\right)\left[\frac{e_a^{sat}(1-h)}{Ta}-C_2\right]. \tag{50}$$

As compared to that over bare soil, the dependence of B on m over plant covered land is more complicated: (a) during the daytime, when $\frac{800}{1+S_0}$ is around one, the impact of m on B is important. The stomatal resistance to vapor transpiration is impacted sensitively during daytime by the soil moisture availability. When the soil moisture availability, m, increases, the value of r_s decreases, based on Eq. (48), which results in a decrement in B, as described by Eq. (45). At night, however, because $S_0=0$, generally we have $\left(\frac{C_1}{m}\right)^2 \ll 800$ when the soil wetness is above its wilting point. Therefore, the influence of m on B over plant covered areas is weak or even disappears at night. The value of B at night is very large based on Eq. (49). The reason seems as following: at night, there is no solar radiation, so there is no photosynthetic activity in the leaves, thus the stomata close, and r_s is much larger than r_a. Therefore transpiration is inhibited based on Eq. (44). H_s, however, is independent of the process mentioned above, which results in a large value of B at night. (b) B over plants is explicitly dependent on turbulent intensity characterized by r_a as expressed by Eq. (45). This is different from that over bare soil where the impact of r_a on B is implicity through the impact of r_a on α and β as described by Eqs. (14) to (18). Equation (45) indicates that the absolute value of B decreases as r_a increases during the day and at night, which, is different to a certain degree, from that over bare soil as shown by Fig. 1. We can anticipate that B over a taller plant canopy has a corresponding larger value. This is because the turbulent intensity over tall vegetation is stronger than that over shorter plants, and (c) the dependence of B on h over a plant canopy is different from that over bare soil. Over bare soil, as indicated by Eqs. (14) and (15), B increases during the day when h increases. Over a plant canopy, however, increasing the value of h, N_p increases but A_p decreases. The compensation results in a weakness of the dependence of B on h over a plant canopy as compared to that over bare soil.

In short, the dependence of B on soil moisture availability and other environmental variables over a plant canopy is more complex than that over bare soil. This is because the evapotranspiration over a plant canopy is not only controlled by turbulent process in the surface layer, but also dominated by r_s. Both r_a and r_s are influenced by the environmental variables mentioned above.

B parameterized through R_N is derived using a procedure similar to that in the derivation over bare soil as:

$$B=\frac{1+A_p\left(\frac{800}{1+S_0}+\frac{c_1^2}{m^2}\right)-N_2}{\frac{LS}{c_p}+N_2}, \tag{51}$$

where N_2 is expressed by Eq. (35) with $\alpha=1$ and $\lambda=0$. Here, over land, completely shielded by vegetation, $G=0$ is assumed. Comparing Eqs. (51) and (34) suggest that the dependence of B on R_N over a plant canopy is similar to that over bare soil.

IV. APPLICATION TO SCALING THE INFLUENCE OF m ON THE INTENSITY OF TIMC

Integrating the one–dimensional potential temperature conservation equation with respect to z and t, from 0 to H and from 0 to τ, respectively, results in:

$$Q=\int_0^H \theta' dZ=\frac{(\theta'_g)^2}{2\beta_0}, \tag{52}$$

$$Q_H=\int_0^\tau \frac{H_s}{\rho cp}dt, \tag{53}$$

where H is the depth of planetary boundary layer (PBL), θ' is the departure from the initial potential temperature (θ'_0), θ'_g is the value of θ' at the surface, β_0 is the background thermal stability defined as $\beta_0=\frac{\partial\theta_0}{\partial z}=$ constant; Eq. (52) was derived by setting $\frac{\partial\theta}{\partial z}=0$.

In a clear sky condition, R_N can be approximately expressed as:

$$R_N=R_{N_0}\sin\left(\frac{\pi t}{T_d}\right), \tag{54}$$

where R_{N_0} is the value of R_N at about noon and T_d is the duration of $R_N>0$. Inserting Eq. (54) into Eq. (5) yields:

$$H_s(t)=H_{s_0}\sin\left(\frac{\pi t}{T_d}\right) \tag{55}$$

with

$$H_{s_0}=\frac{(1-\lambda)R_{N_0}}{1+B}. \tag{56}$$

Substituting Eq. (55) into Eq. (53) results in:

$$Q_H(\tau)=\frac{H_{s_0}T_d}{\pi}\left(1-\cos\frac{\pi\tau}{T_d}\right). \tag{57}$$

Assuming that D is the characteristic scale of a wetter area, U is the characteristic wind speed, and T_c is the characteristic time scale, expressing air moving from the center of the wetter area to its surrounding then:

$$T_c=\frac{D}{2U}. \tag{58}$$

The buoyancy excess over a drier area in the PBL during the period from t_0, to T_c+t_0

can be derived from Eqs. (52), (53), and (57):

$$\frac{g}{\theta}(\Delta Q_d - \Delta Q) = A\frac{gT_d}{\pi\theta_0}\left(H^d_{s_0} - H_{s_0}\right)\left[\cos\left(\frac{\pi t_0}{T_d}\right) - \cos\frac{\pi(t_0 - T_c)}{T_d}\right] \tag{59}$$

with $0 \leqslant T_0 < T$ and $\Delta Q = Q(t_0 + T_c) - Q(t_0)$, where the sub– or super–script d in Eq. (59) expresses the value for the drier area; $A \leqslant 1$ is a coefficient considering air mixing processes in the frontal zone.

The characteristic wind speed of TIMC, U_c, can be scaled by assuming the work done by the buoyancy force is used to create kinetic energy:

$$U_c = \left[A\frac{2gT_d}{\pi\theta_0}\left(H^d_{s_0} - H_{s_0}\right)\left(\cos\frac{\pi t_0}{T_d} - \cos\frac{\pi(t_0 + T_c)}{T_d}\right)\right]^{1/2}. \tag{60}$$

Equation (60) indicates that the intensity of TIMC is proportional to the square root of the excess sensible heat flux. When m_g increases (which results in the contrast increase between the wetter area and its surroundings), the value of B decreases non–linearly as described in Fig. 3a and R_{N_0} increases as shown by Eq. (42), suggesting an increase of U_c as related to an increase in the contrast of m. Any environment influencing the value of B as discussed above will impact the value of U_c based on Eqs. (56) and (60).

Equation (60) also describes that the perturbed area scale influences the U_c non–linearly: U_c non–linearly increases with increasing T_c (i.e., D) under the conditions $T_c < T_d$. After $T_c \geqslant T_d$, the variation in T_c (or D) will not impact U_c anymore.

V. CONCLUSIONS

In the present study, a new parameterization formulation of Bowen ratio over non–vegetation covered ground surface was derived. The study also briefly investigated the Bowen ratio over vegetation covered areas. The major conclusions we obtained from this study are as follows:

- The Bowen ratio depends on six variables, including soil volumetric fraction of porosity, soil moisture availability, the resistance ratio between air and within soil pores, atmospheric thermal stability, atmospheric relative humidity, and temperature.
- The Bowen ratio over a ground surface is not a continuous function. The singularity of Bowen ratio occurs at $\alpha h_c = h$, with $\alpha = 1$ both over free water and a vegetation canopy. The singularity separates $B > 0$ from $B < 0$. $B \to \infty$ when $\alpha h_c - h \to 0$. The singularity can occur more easily under the following conditions: at night, weak atmospheric turbulence, over dry soil, high relative humidity in the air, and a stable stratified atmosphere.

In the following conclusions, the case with a singularity is not included.

- For a fixed soil moisture availability and uniformly distributed soil type, the Bowen ratio is inversely proportional to soil volumetric fraction of porosity.
- The Bowen ratio is approximately independent of $\frac{r_a}{r_D}$ during the day and slowly decreases at night as the resistance ratio between the air and the soil pores increases.
- The Bowen ratio is inversely proportional to soil moisture availability where the resistance ratio is on the order of $0(10^{-2})$ and / or the soil moisture availability is not less than its field capacity. For other conditions, a deviation of the Bowen ratio from being inversely proportional to soil moisture availability occurs. The difference increases as soil becomes dry and / or the resistance ratio increases.

• When the relative humidity of air increases, the value of the Bowen ratio increases during the day but decreases at night.

• Increasing temperature results in a decrease of the absolute value of the Bowen ratio during the day and at night. It suggests that the Bowen ratio has an annual cycle with its maximum value in the winter season. This ratio varies with latitude and altitude with relatively larger values in higher latitudes and over highlands.

• The impact of atmospheric thermal stability on the Bowen ratio is complex.

• When the absolute value of net radiation at the surface increases, the absolute value of the Bowen ratio also increases. The turbulent resistance will respond to the variation of the net radiation at the surface. During the day, the influence of the resistance on the Bowen ratio is opposite to that at night.

• The Bowen ratio over a vegetation covered area is larger than that over a free water surface by a factor of $\left(1+\frac{r_s}{r_a}\right)$. The difference of Bowen ratios over a vegetation canopy and a free water surface decreases as $\frac{r_s}{r_a}$ reduces. Some differences between the Bowen ratios over bare soil and over vegetation canopy are caused by different reactions to the environment variations between them: (a) during the day, the Bowen ratio is approximately independent of the air resistance over bare soil, but is reduced over a canopy when air resistance increases, and (b) the Bowen ratio responds to the variation of atmospheric relative humidity in a weaker manner over a vegetation covered area as compared to that over bare soil, because of the leaf stomatal resistance decreases as atmospheric relative humidity increases.

• The impact of Bowen ratio on the intensity of thermally induced mesoscale circulation is scaled by Eqs. (14), (15), (56), and (60). The above discussions can be used to estimate the circulation intensity impacted by the above mentioned elements whe the surface net radiation flux is known.

IV. APPENDIX

Lists of Symbols

A	= surface albedo over bare soil
A_{min}	= the minimum value of A
A_p	= defined by Eq. (52)
B	= Bowen's ratio
B_*	$=\chi_p B$
B_{max}	= the maximum value of B
C_1 and C_2	= parameters related to Eq. (50)
c_p	= specific heat at constant pressure
D	= the characteristic scale of wetter area
G	= soil heat flux
H	= the depth of PBL
h	= relative humidity in the lower surface layer
h_{cb}	$=q_r^{sat}/q_a^{sat}$
h_{sp}	$=q_p^{sat}/q_a^{sat}$
h_s	= the relative humidity in soil pores

H_s = sensible heat flux

K_a = diffusivity of heat or water vapor

L = latent heat

LAI = leaf area index

LE = latent heat flux

m = soil moisture availability defined by Eq. (8)

m_c = $\dfrac{A_d - A_{\min}}{\alpha_m}$

m_{fc} = value of m at field capacity

m_{wilt} = value of m at a wilting point for plants

N_b = defined by Eq. (15)

N_p = defined by Eq. (48)

N_1 = defined by Eq. (37)

N_2 = involved in Eq. (53)

q = specific humidity

$R_L^{\uparrow}$ = upward longwave radiation flux

$R_L^{\downarrow}$ = downward longwave radiation flux

R_N = net radiation flux at surface

R_{N_0} = the value of R_N at noon

R_s = solar radiation observed by surface

r_a = resistance to the exchange of sensible or latent heat flux in air

r_D = resistance to the vapor diffusion in soil pores

r_s = stomatal resistance against vapor transpiration

S = slope of the saturation vapor versus temperature curve

S_0 = incoming solar radiation

T = temperature

TIMC = thermally induced mesoscale circulation

T_c = characteristic time scale

T_d = duration of $R_N > 0$

U = characteristic wind speed

U_c = the intensity of TIMC

Q = $\int_0^H \theta' dZ$

$Q_H(\tau)$ = $\int_0^{\tau} \dfrac{H_s}{\rho c p} dt$

Z_a = height above surface

α = defined by Eq. (18)

α_m = a constant involved in Eq. (7)

α_s = defined by Eq. (41)

β = defined by Eq. (16)

β_* = defined by Eq. (17)

ΔZ_0 = a very thin upper soil layer

ΔZ_1 = a thin soil layer next to ΔZ_0

ε = an infinitesimal value

ε_a = air emissivity

ε_g = surface emissivity
θ_0 = background potential temperature
θ' = the departure from θ_0
λ = partition of R_N into G
ρ = air density
η_w = soil volumetric water fraction
χ_p = volumetric fraction of soil pores

Subscripts.

g = the value within ΔZ_0
1 = the value within ΔZ_1
s = the value at surface
a = the value in lower surface layer
d = the value at absolute dry soil condition

Superscripts.

sat = at saturation condition

This study was supported by NSF grant #ATM-8915265 and NSF grant #ATM-9306754. Ye Zhuojia acknowledges the support of the Chinese NNSF. We would like to thank T. Smith, B. Critchfield, and D. McDonald for the preparation of this manuscript, and thanks to Dr. Zeng X. for the preparation of the Figures. D. McDonald is also acknowledged for very carefully editing the text of the paper.

REFERENCES

Ching, J.K.S. (1985), Urban-scale variations of turbulence parameters and fluxes, *Bound.-Layer Meteor.*, **33:** 335-361.

Ching, J.K.S., Clarke, J.F., and Godowitch, J.M. (1983), Modulation of heat flux by different scales of advection in an urban environment, *Bound.-Layer Meteor.*, **25:** 171-191.

Deardorff, J.W. (1978), Efficient prediction of ground surface temperature and moisture with inclusion of a layer of vegetation, *J. Geophys. Res.*, **83:** 1889-1903.

Idso, S.B., Jackson, R.D., Kimball, B.A., and Nakayma, F.S. (1975), Dependence of bare soil albedo on soil water content, *J. Appl. Meteor.*, **14:** 109-113.

Jacquemin, B., and Noilhan, J. (1990), Sensitivity study and validation of land surface parameterization using the HAPEX-MOBILHY data set, *Bound.-Layer Meteor.*, **52:** 93-134.

Kalanda, B.D., Oke, t.B., and Spittlehouse, D.L. (1980), Suburban energy balance estimates for Vancouver, B.C. using the Bowen ratio-energy balance approach, *J. Appl. Meteor.*, **19:** 791-802.

Lee, T.J. and Pielke, R.A. (1992), Estimating the soil surface specific humidity, *J. Appl. Meteor.*, **31:** 480-484.

Mahrer, Y. and Pielke, R.A. (1977), A numerical study of the airflow over irregular terrain, *Beitrage zur Physik der Atmosphare*, **50:** 98-113.

McCaughey, J.H. (1985), A radiation and energy balance study of mature forest and clearcut sites, *Bound.-Layer Meteor.*, **32:** 1-24.

McNider, R.T. and Pielke, R.A. (1981), Diurnal boundary layer development over sloping terrain, *J. Atmos. Sci.*, **38:** 2198-2212.

Nappo, C.J. (1975), Parameterization of surface moisture and evaporation rate in planetary boundary layer model, *J. Appl. Meteor.*, **14:** 289-296.

Nunez, M. and Oke, T.R. (1977), The energy balance of an urban canyon, *J. Appl. Meteor.*, **16:** 11-19.

Oke, T.B. (1982), The energetic basis of the urban heat island, *Quart. J. Roy. Meteor. Soc.*, **108:** 1–24.

Segal, M., Jia, X., Ye, Z., and Pielke, R.A. (1990), On the effect of daytime surface evaporation on pollution dispersion, *Atmos. Environ.*, **24A:** 1801–1811.

Segal, M., Kallos, G., Brown J., and Mandel, M. (1992), Morning temporal variations of shelter–level specific humidity, *J. Appl. Meteor.*, **31:** 74–85.

Segal, M. and Arritt, R.W. (1992), Non–classical mesoscale circulations caused by surface sensible heat flux gradients, *Bull. Amer. Meteor. Soc.*, **73:** 1593– 1604.

Singh, B., Vian A., and Guehi, G. (1985), *Stomatal resistance of a hardwood forest as related to meteorological parameters*, 17th Conference Agricultural and Forest Meteorology and 17th Conference Biometeorology and Aerobiology, 239– 243.

Smith, E.A., Reiter, E.R., and Gao, Y. (1986), Transition of surface energy budget in the Gobi desert between spring and summer seasons, *J. Appl. Meteor.*, **25:** 1725–1740.

Ye., Z., and Pielke, R.A. (1993), Atmospheric parameterization of evaporation from non–plant–covered surfaces, *J. Appl. Meteor.*, **32:** 1248–1258.